Experimental Comparison of ALO and MRAS Speed Observers for Induction Motors

Denis Panxhi[1], Aida Spahiu[1], Nuri Rusta[1], and Donald Selmanaj[1]

***Abstract*— Induction motors (IM) are an integral part of various industrial applications due to their durability, reliability, and efficiency. Therefore, accurate speed observation of these motors is essential for optimizing performance, operational safety, and increased energy efficiency. This paper presents an experimental comparison of two-speed observation techniques such as the Adaptive Luenberger Observer (ALO) and the Model Reference Adaptive System (MRAS). The experimental setup includes a high-voltage platform for the motor speed controller and actual speed, voltage, and current measurements. At different motor speeds, measurements are taken to analyze and evaluate the accuracy and performance of each method. The results show small variations in the performance of these techniques and minor deviations from the the measured motor speed. This comparative analysis provides valuable insights into choosing the appropriate speed observation method for specific applications. A thorough conclusion is provided, discussing the advantages and disadvantages of each technique.**

I. INTRODUCTION

Driven by the need to eliminate the problems related to speed sensors such as minimizing maintenance requirements, reducing costs, and improving reliability, various observers for IM have been analyzed and discussed in the Scientific Literature. Various observer techniques are explained in different papers that are widely recognized for their universality and versatility. These methods are mainly based on the IM model expressed in the $\alpha\beta$ or the dq reference frame. Increasing the sensorless control performance of the IM has special attention due to the higher utilization in different industrial sectors. The control performance is directly dependent on the performance of the estimation algorithm. On the other hand, the performance of the estimation algorithm is directly dependent on the electrical parameters of IM, especially in the stator and rotor resistances [1]. These are dependent on the temperature and frequency, which affect the estimation algorithm performance. Different speed observers like ALO and MRS contain a speed adaptation mechanism [1] which is derived using the state-error equations and the Lyapunov stability theorem. The estimated speed depends on the accuracy of IM parameters, especially stator and rotor resistance, and an adaptive estimation method of stator resistance is used to eliminate its influence. Different Luenberger observers are discussed and analyzed in the literature [2] - [7]. Luenberger's methods proposed in these papers have gained attention due to their accuracy in estimating the state of IM in dynamic and steady states, where estimated states are used in sensorless control applications. The flexibility of Luenberger observers allows them to be easily implemented into IM, making the observer the most used to estimate the IM states. Their easy implementation and ability to provide a correct state estimation, especially the rotor speed, make the Luenberger observer one useful alternative for sensorless IM control. The Luenberger observer usually operates in the dq reference frame [2], [4], and [5] with an adaptive mechanism to estimate the rotor speed of IM. However, other papers such as [3] apply the $\alpha\beta$ reference frame for IM speed estimation. The work in [6] presents a method to choose the proportional coefficient between the eigenvalues to the IM and Luenberger observer to ensure stability in both IM and regeneration mode running. The paper [7] presents a method that uses a state observer based on the Lyapunov function for deterministic evaluation of the states, with its effectiveness proven experimentally. An alternative to ALO are the MRAS algorithms, proposed in different works, [8]-[16]. One main advantage of MRAS algorithms is the wide range of speeds they can perform. Different papers highlight the fact that the MRAS algorithm is an effective method to estimate rotor speed due to dynamic and static performance, stability, and simplicity. Methods in [9] and [12] describe the MRAS algorithm on dq reference frame where the [9] explains the torque model reference adaptive schemes (TMRAS) to improve the performance on low speed and solve the problems of pure integrator, and on [12] is presented the MRAS algorithm as a classical solution. Other works, [14] and [16], propose a Neural Network (NN) as an adaptive model on the MRAS algorithm. In [13] a classical MRAS algorithm is presented where the pure integrator is replaced with a low-pass filter to improve the performance on low speed, and in [8] an MRAS for IM using instantaneous reactive power is proposed where the poor performance due to pure integrator and stator resistance is highlighted. Different MRAS models like rotor flux-based MRAS, and back e.m.f-based MRAS, have been proposed and compared on [15], where advantages and disadvantages are highlighted. An MRAS estimator has been proposed on [11] where the rotor position is calculated by a special algorithm that eliminates the PI controller of the adaptation mechanism, and in [10] where the adaptation algorithm is modified, and a new adaptation algorithm different from classical solutions is introduced.

The paper is structured as follows: Section II provides the IM model. Section III introduces the ALO, while Section IV introduces the MRAS observer. In section V, the results

[1]D. Panxhi, A. Spahiu, N. Rusta, and D. Selmanaj are with the Faculty of Electrical Engineering, Polytechnic University of Tirana, "Mother Tereza" Square, Nr. 4, Tirana, Albania denis.panxhi@upt.al, aida.spahiu@fie.edu.al, nuri.rusta@fie.edu.al, donald.selmanaj@upt.al

of the experimental comparison are presented and analyzed. The paper ends with conclusions in Section VI.

II. INDUCTION MOTOR MODEL

Various mathematical models are used to estimate the rotor speed of an IM. The adaptive Luenberger observer is applied to the IM's state space and velocity model. The MRAS observer is built on the reference model and adaptive model of the IM, where the states of the reference model are compared with the states of the adaptive model, and the difference between states is used by the adaptation mechanism.

A. State space model of IM

The model is expressed on the stator fixed reference frame $(\alpha\beta)$ by assuming the stator currents and rotor fluxes as state variables. The state-space representation of the IM is given by:

$$\begin{aligned} \frac{dX(t)}{dt} &= AX(t) + BU(t) \\ Y(t) &= CX(t), \end{aligned} \tag{1}$$

where X, U, and Y are the state vector, the input vector, and the output vector, respectively. A is the system matrix, B is the input matrix, and C is the output matrix. Furthermore, $i_{s\alpha}$ and $i_{s\beta}$ are stator currents, $\psi_{r\alpha}$ and $\psi_{r\beta}$ are rotor fluxes, and $u_{s\alpha}$ and $u_{s\beta}$ are stator voltages, all in the $\alpha\beta$ reference frame.

$$X = \begin{bmatrix} i_{s\alpha} \, i_{s\beta} \, \psi_{r\alpha} \, \psi_{r\beta} \end{bmatrix}^t, \; U = \begin{bmatrix} u_{s\alpha} \, u_{s\beta} \end{bmatrix}^t, \; Y = \begin{bmatrix} i_{s\alpha} \, i_{s\beta} \end{bmatrix}^t$$

$$A = \begin{bmatrix} \alpha_{11} & 0 & \alpha_{12} & -\alpha_{13}\omega_r \\ 0 & \alpha_{11} & \alpha_{13}\omega_r & \alpha_{12} \\ \alpha_{21} & 0 & \alpha_{22} & -\alpha_{23}\omega_r \\ 0 & \alpha_{21} & \alpha_{23}\omega_r & \alpha_{22} \end{bmatrix}, \qquad B = \begin{bmatrix} \beta & 0 \\ 0 & \beta \\ 0 & 0 \\ 0 & 0 \end{bmatrix}$$

$$C = \begin{bmatrix} 1 & 0 & 0 & 0 \\ 0 & 1 & 0 & 0 \end{bmatrix}.$$

The parameters of matrices A and B are the following.

$$\alpha_{11} = -\left(\frac{1}{\sigma\tau_s} + \frac{1-\sigma}{\sigma} \cdot \frac{1}{\tau_r} \right), \; \alpha_{12} = \frac{L_m}{\sigma L_s L_r} \cdot \frac{1}{\tau_r}$$

$$\alpha_{13} = -\frac{L_m}{\sigma L_s L_r}, \; \alpha_{21} = \frac{L_m}{\tau_r}, \; \alpha_{22} = -\frac{1}{\tau_r}, \; \alpha_{23} = 1$$

$$\tau_r = \frac{L_r}{R_r}, \quad \tau_s = \frac{L_s}{R_s}, \quad \sigma = 1 - \frac{L_m^2}{L_s L_r}, \quad \beta = \frac{1}{\sigma L_s}$$

where, R_s and R_r represent the stator and rotor resistance, L_s and L_r are the respective stator and rotor inductance, τ_s and τ_r are the stator and rotor time constants, L_m is the mutual inductance, σ is the leakage or coupling factor.

B. MRAS model of IM

Reference model

MRAS-based algorithms use a reference model of the IM, formed from two models: the voltage model (stator model) and the current model (rotor model). For high speed, the voltage model is utilized whereas the current model is designed for low-speed operations. The reference model uses a PI controller to provide a smooth transition between the outputs of the two models.

Voltage model

The voltage model is represented in the stator reference frame $(\alpha\beta)$, from which the stator flux and the rotor flux without a speed signal are estimated.

$$\begin{aligned} \vec{\psi}_{s\alpha\beta} &= \int \left[\vec{u}_{s\alpha\beta} - R_s \vec{i}_{s\alpha\beta} \right] dt \\ \vec{\psi}_{r\alpha\beta} &= \frac{L_r}{L_m} \left[\vec{\psi}_{s\alpha\beta} - \sigma L_s \vec{i}_{s\alpha\beta} \right], \end{aligned} \tag{2}$$

where $\vec{\psi}_{s\alpha\beta} = \psi_{s\alpha} + j\psi_{s\beta}$ ($\vec{\psi}_{s\alpha\beta}$ is the stator flux vector in the $\alpha\beta$ reference frame), $\vec{\psi}_{r\alpha\beta} = \psi_{r\alpha} + j\psi_{r\beta}$, $\vec{u}_{s\alpha\beta} = u_{s\alpha} + ju_{s\beta}$, and $\vec{i}_{s\alpha\beta} = i_{s\alpha} + ji_{s\beta}$.

Current model

The current model is based on the differential equations of the rotor. Model (3) is expressed in the dq rotating reference frame, where the dq frame rotates at the rotor speed ω_r.

$$\frac{d\vec{\psi}_{rdq}}{dt} = -\frac{1}{\tau_r}\vec{\psi}_{rdq} + \frac{L_m}{\tau_r}\vec{i}_{sdq}, \tag{3}$$

where $\vec{\psi}_{rdq} = \psi_{rd} + j\psi_{rq}$, and $\vec{i}_{sdq} = i_{sd} + ji_{sq}$ ($\vec{\psi}_{rdq}$ and $\vec{i}_{sdq}$ are defined as rotor flux and stator current vectors, respectively, in the dq reference frame).

Adaptive model

The adaptive MRAS model from which the adjustable rotor flux is provided is given by the equation (4):

$$\frac{d\vec{\psi}_{r\alpha\beta}}{dt} = \frac{L_m}{\tau_r}\vec{i}_{s\alpha\beta} + \left[j\omega_r - \frac{1}{\tau_r} \right] \vec{\psi}_{r\alpha\beta}. \tag{4}$$

The reference and adaptive models of MRAS are compared to generate an error flux used as input of a PI controller to adjust the rotor speed ω_r.

III. ADAPTIVE LUENBERGER OBSERVER

The Luenberger observer is very useful in control systems, as it estimates states of an observable system when it is impossible to measure these states and enhances the system control. The observer gain matrix L is crucial, directly affecting the stability and accuracy of system state estimates and control performance. The proper design of the matrix L ensures that the state of the system is effective and accurate.

Discrete model

The implementation of the Luenberger observer requires the discretization of machine equations. The discrete equations can be obtained from equation (1).

$$\begin{aligned} X(k+1) &= A_d X(k) + B_d U(k) \\ Y(k) &= C_d X(k), \end{aligned} \tag{5}$$

where $X(k)$ is the state vector at step k, $U(k)$ is the input vector at step k, and $Y(k)$ is the output vector at step k. The discretized matrices, the system matrix A_d, the input matrix B_d, and the output matrix C_d using the Euler methods are:

$$A_d = \begin{bmatrix} \alpha_{11}T_s + 1 & 0 & \alpha_{12}T_s & -\alpha_{13}\omega_r T_s \\ 0 & \alpha_{11}T_s + 1 & \alpha_{13}\omega_r T_s & \alpha_{12}T_s \\ \alpha_{21}T_s & 0 & \alpha_{22}T_s + 1 & -\alpha_{23}\omega_r T_s \\ 0 & \alpha_{21}T_s & \alpha_{23}\omega_r T_s & \alpha_{22}T_s + 1 \end{bmatrix}$$

$$B_d = \begin{bmatrix} \beta T_s & 0 \\ 0 & \beta T_s \\ 0 & 0 \\ 0 & 0 \end{bmatrix} \qquad C_d = \begin{bmatrix} 1 & 0 & 0 & 0 \\ 0 & 1 & 0 & 0 \end{bmatrix},$$

where T_s is the sampling time.

Observer design

The overall architecture of the adaptive Luenberger observer is shown in Fig. 1, where the adaptation mechanism calculates the rotor speed. The ALO estimates the state vector $\hat{X}(k)$ of an observable system using the discrete equations (6).

$$\begin{aligned} \hat{X}(k+1) &= A_d\hat{X}(k) + B_dU(k) + L_d\left[Y(k) - \hat{Y}(k)\right] \\ \hat{Y}(k) &= C_d\hat{X}(k), \end{aligned} \tag{6}$$

where, $\hat{X}(k)$ is the estimated state vector at step k, $\hat{Y}(k)$ is the estimated output vector at step k, and L_d is the discretized observer gain matrix. The rotor speed is evaluated by the adaptation mechanism [1] where the PI controller calculates the speed based on input error. The adaptation mechanism is designed to achieve system stability by using the state error dynamic equations and Lyapunov's stability theorem. The following equation (7) represents the dynamics of the estimation error:

$$e(k+1) = [A_d - L_dC_d)]e(k), \tag{7}$$

where $e(k)$ represents the error vector at step k.

The observer error converges to zero if equation (7) is stable, therefore if the eigenvalues of $(A_d - L_dC_d)$ are within the unit circle. The value of L_d should be such that the transient response of the observer must be faster than the controlled closed-loop response to yield a rapidly updated estimate of the state vector. The gain matrix L_d is chosen to minimize the estimation error during the dynamic and static regions. One approach to achieving this is calculating the coefficient of L_d proposed by [1].

Speed adaptation law

The adaptation mechanism estimates the rotor speed ω_r by taking the estimated rotor fluxes $\psi_{r\alpha}, \psi_{r\beta}$ from ALO and output errors ($e_{is\alpha} = i_{s\alpha} - \hat{i}_{s\alpha}$ and $e_{is\beta} = i_{s\beta} - \hat{i}_{s\beta}$) [1]. The PI controller error can be calculated by combining the estimated fluxes and output errors by equation (8):

$$\hat{e} = e_{is\alpha}\hat{\psi}_{r\beta} - e_{is\beta}.\hat{\psi}_{r\alpha}. \tag{8}$$

Based on the error expression (8) the rotor speed $\hat{\omega}_r$ is estimated with the help of a PI controller [1].

$$\hat{\omega}_r = K_P\hat{e} + K_I\int \hat{e}\,dt. \tag{9}$$

The discrete equation of the rotor speed expression (9) is obtained using Euler's method.

$$\hat{\omega}_r(k) = \hat{\omega}_r(k-1) + K_P\left[\hat{e}(k) - \hat{e}(k-1)\right] + K_iT_s\hat{e}(k-1). \tag{10}$$

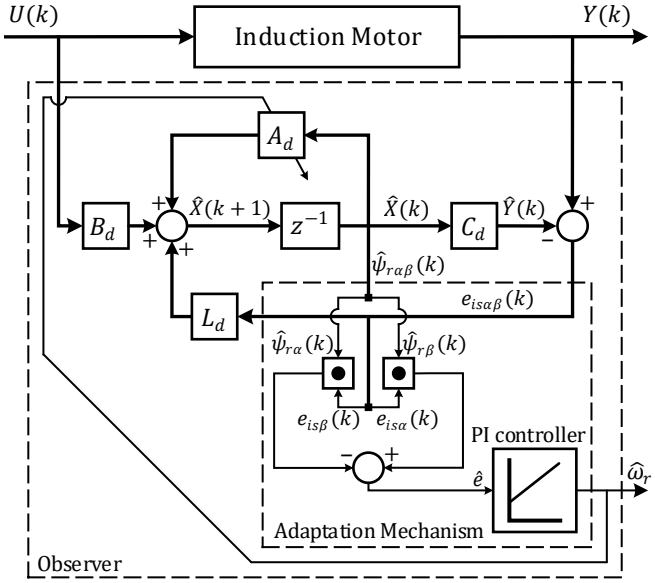

Fig. 1. Structure of adaptive Luenberger observer.

IV. MRAS OBSERVER

The MRAS observer for an IM uses two independent models (Reference model and Adaptive model) to estimate the same variable based on the same inputs. The rotor speed $\hat{\omega}_r$ is estimated by adaptation block such as [1] and [13].

Reference model

The reference model structure Fig. 2 is built based on equations (2) and (3), which are two different mathematical models that calculate the same state variables [13]. Below the Fig. 2 illustrates the reference model that calculates the rotor flux $\vec{\psi}_{r\alpha\beta}$ and angle position $\theta_{r\alpha\beta}$ from the measurement signals $\vec{u}_{r\alpha\beta}$ and $\vec{i}_{r\alpha\beta}$. The reference model includes the voltage model for high-speed operations and the current model for low-speed operations [13].

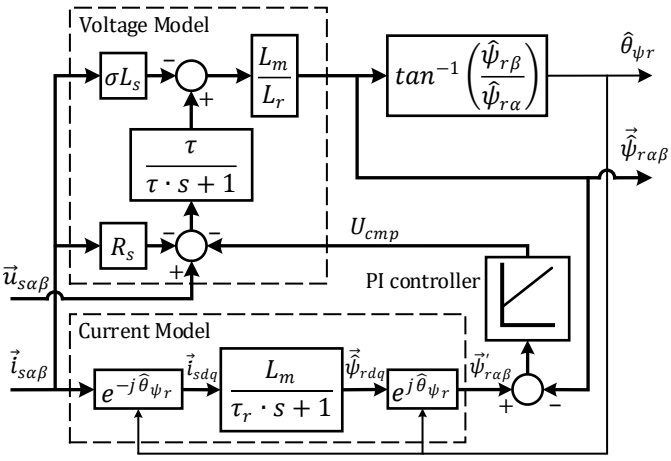

Fig. 2. Structure of reference model

A PI controller is used to compensate for the mismatch in estimation between the two models. The voltage model (2)

that calculates the rotor flux without a speed signal contains a pure integrator, which brings poor performance at low-speed operations [1], [8] and [9]. The pure integration is approximated by a low-pass filter to avoid issues related to pure integration and performance and is given by (11):

$$\frac{1}{s} \approx \frac{\tau}{\tau s + 1}, \qquad \tau = 1/2\pi f, \qquad f = 0.5Hz. \tag{11}$$

Fig. 2 compares the rotor flux from the current model with the rotor flux of the voltage model and produces a flux error, which is an input for a PI controller. The PI controller produces a compensated voltage based on the flux error to achieve a smooth transition between models.

Speed observer

Fig. 3 shows the adaptive model by which the rotor flux is adjusted due to rotor speed.

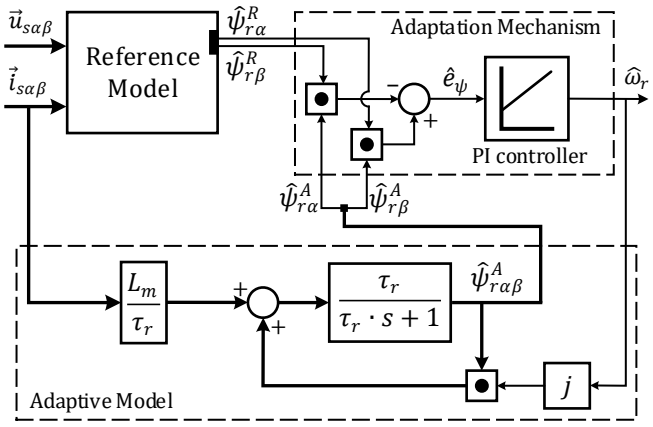

Fig. 3. Structure of MRAS speed observer

The MRAS speed observer uses an adaptation mechanism that incorporates the rotor flux error by comparing the output of the models and the PI controller to calculate the rotor speed $\hat{\omega}_r$. The output of the adaptive model is represented in the stator reference frame ($\alpha\beta$) and is compared with the output of the reference model to produce flux error. The flux error is expressed by equation (12).

$$\hat{e}_\psi = \vec{\hat{\psi}}^R_{r\alpha\beta} \times \vec{\hat{\psi}}^A_{r\alpha\beta} = \hat{\psi}^R_{r\alpha}\hat{\psi}^A_{r\beta} - \hat{\psi}^R_{r\beta}\hat{\psi}^A_{r\alpha}. \tag{12}$$

The rotor flux error $\hat{e}_\psi$ for the PI controller is determined by the cross-product of output fluxes from reference and adaptive models. The PI controller is part of the adaptation block which calculates the rotor speed (13) as its output based on the minimization of its input flux error.

$$\hat{\omega}_r = K_P \hat{e}_\psi + K_I \int \hat{e}_\psi \, dt. \tag{13}$$

The discrete equation of the rotor speed expression (13) is given by equation (14).

$$\hat{\omega}_r(k) = \hat{\omega}_r(k-1) + K_P\left[\hat{e}_\psi(k) - \hat{e}_\psi(k-1)\right] + K_i T_s \hat{e}_\psi(k-1). \tag{14}$$

V. EXPERIMENTAL COMPARISON RESULTS

Here the two algorithms are compared on an experimental setup. The experiments for both methods ALO and MRAS are realized on identical conditions. To verify the performance of these methods, the estimated speeds are compared with the actual measured speed for IM. Also, the speed estimation error is calculated as a difference between the measured and estimated speed ($\Delta\omega = \omega_r - \hat{\omega}_r$). The speed error is used as a performance indicator on both the transient and steady-state of the rotor speed. The speed error is used to identify which observer performs better in different conditions, highlighting strengths and weaknesses in their ability to estimate speed accurately. Also, a comparison in terms of Root Mean Square Error (RMSE) is treated to determine the differences between observed values and actual values. The RMSE is calculated for various speed references ranging from 25 rad/s to 90 rad/s, providing significant information in terms of speed estimation accuracy for different speed operations. The rated values and parameters of the IM used in the experiments are presented in the following tables.

The rated values of the IM

P [kW]	U [V]	I [A]	n [rpm]	T [Nm]	p_p
0.55	220	1.8	870	6.04	3

The parameters of the IM

R_s [Ω]	R_r [Ω]	L_s [H]	L_r [H]	L_m [H]	J_T [kg.m^2]	T_m [s]
12.98	14.17	0.655	0.655	0.61	0.0021	0.654

In the case of ALO, the rotor speed estimate will converge quickly if the K_i is sufficiently large and K_p is relatively small. In our experimental results, the coefficients are $K_i = 6910$ and $K_p = 5$. Increasing the K_p will result in speed fluctuation and increase transient and steady-state error. For the MRAS if the Kp and Ki are sufficiently large the rotor speed estimate will converge quickly. In our experimental results, the coefficients are $K_i = 11570$ and $K_p = 33655$.

A. No load test

Fig. 4 shows the measured voltage and current in the $\alpha\beta$ reference frame during the no-load test. In Fig. 4 the transition phase is observed from 0 to 0.4 s, clearly illustrating the current diagram where the current arrives at the maximum of 1 A and the voltage reaching a maximum of 100 V. After this transition the steady state occurs approximately at 0.25 s where the current is 0.5 A and the voltage at 90 V. After the steady period, another transition occurs, which start at 0.65 s and ends at 0.8 s approximately where the maximum current is 0.65 A.

Fig. 5 shows the results of the no-load test, in which the speeds from the ALO and MRAS algorithms are compared to the real measurement speed ω_r, as well as the speed error between observers and real speed.

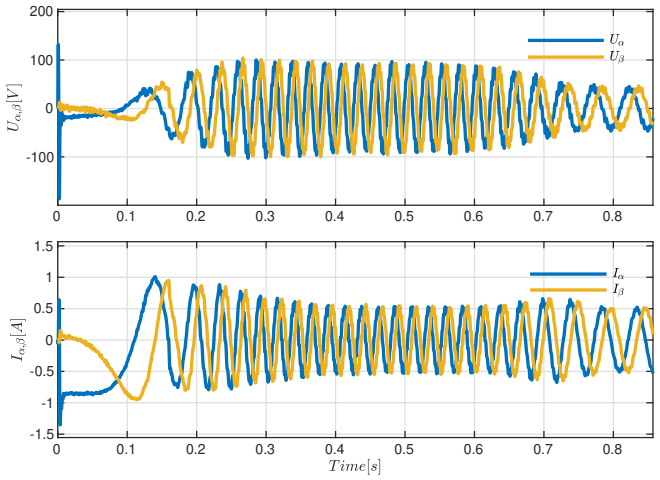

Fig. 4. Voltage and current curves during the no-load test.

In the initial phase from 0 to 0.4 s, the speed is increased from 0 to 84 rad/s. After that, the speed remains constant for approximately at 0.2 s at 84 rad/s, and this is followed by the final phase where the speed is decreased from 84 rad/s to 40 rad/s.

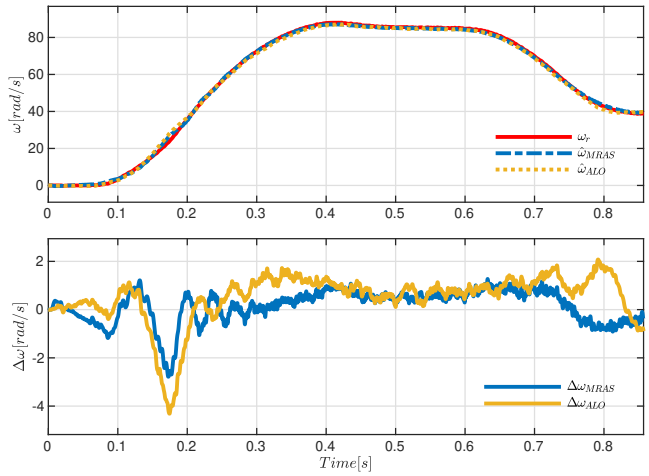

Fig. 5. Speed and error curves during the no-load test.

Transient Performance: In the transient phase, the MRAS shows better performance compared to ALO, this is easily evident because the error speed of MRAS is smaller than the ALO. The MRAS demonstrates a better transient response, adapts more effectively, and has more precision in tracking the real speed ω_r.

Steady State Performance: Both methods demonstrate similar performance in steady state. This suggests that the MRAS and ALO observers offer the same performance in maintaining accuracy when the speed is stable.

Fig. 6 shows the RMSE plot where the MRAS performs better compared to ALO for a speed range between 25 rad/s to 90 rad/s. The small RMSE values in this range for MRAS compared to ALO indicate that MRAS has a more accurate speed estimation than ALO.

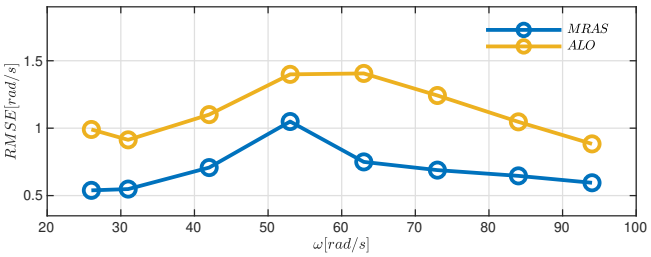

Fig. 6. Performance in terms of RMSE

B. Load test

Fig. 7 shows the measured voltage and current in the $\alpha\beta$ reference frame during the load test. In Fig. 7 the transition phase is shown from 0 to approximately 0.3 s, during which the voltage arrives at the maximum of 170 V and the current arrives at the maximum of 1.9 A. Following this transition, the steady state is presented at approximately 0.3 s where the current is 1.5 A and the voltage at 170 V. After the steady period, another transition occurs, which starts at 0.6 s and ends at 0.77 s, where the current starts to decrease and arrives a minimum of 1 A and at the end of transition achieves a new state with 1.45 A and a voltage of 110 V.

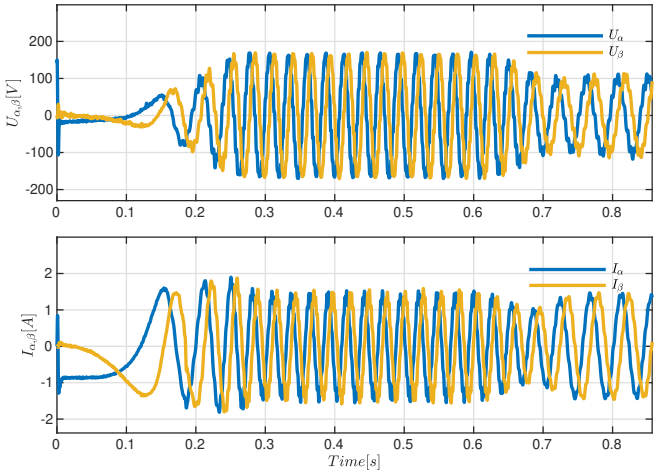

Fig. 7. Voltage and current curves during the load test.

Fig. 8 shows the results with load test, where the speeds from the ALO and MRAS algorithms are compared with real measurement speed ω_r, as well as the speed error between observers and real speed. In the initial phase from 0 to 0.4 s, the speed is increased from 0 to 73 rad/s. After that, the speed remains constant at 73 rad/s for approximately 0.2 s. This is followed by the final phase where the time is greater than 0.6 s and the speed decreases from 73 rad/s to 40 rad/s.

Transient Performance: Both the MRAS and ALO show similar performance in terms of oscillations, stability, and accuracy. The oscillations show that the two methods have comparable performance in speed variations and almost the same speed accuracy. The similarities suggest that both observers perform equally well during dynamic conditions, maintaining stability and robustness even under rapidly

changing operating scenarios. These results demonstrate their suitability for sensorless control applications where robustness and accuracy are essential.

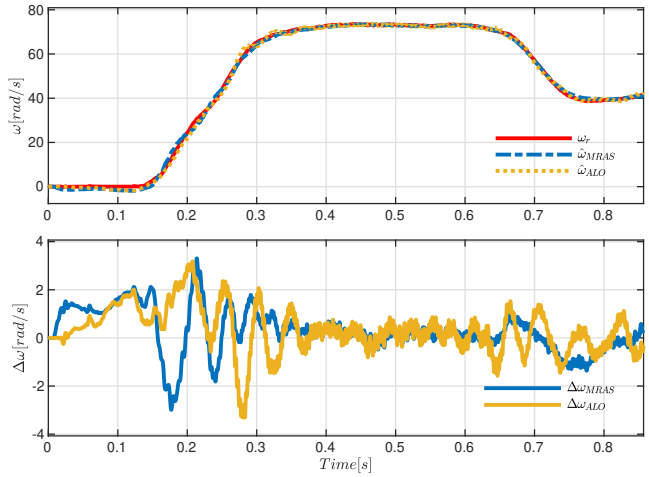

Fig. 8. Speed and error curves during the load test.

Steady State Performance: Both methods show comparable performance in the steady state, with the speed error being quite identical. However, the error amplitude for ALO is slightly greater than that of MRAS. This shows that both observers are effective in the stable state, but MRAS offers a slightly narrower error range.

Fig. 9 presents the RMSE plot in which both MRAS and ALO perform with a little difference in RMSE values across the speed range of 25 rad/s to 90 rad/s.

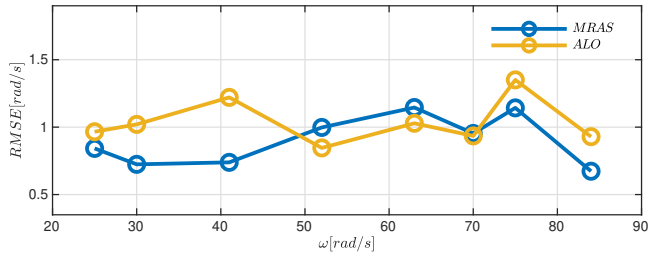

Fig. 9. Performance in terms of RMSE

The small difference in RMSE values indicates that the MRAS and ALO offer similar accuracy within this speed range.

VI. CONCLUSION

This paper introduces a comparison of two speed observers used for IM, such as MRAS and ALO. It presents a comparison of real speed with observed speeds with no-load and load tests and highlights the performance of each observer. The analysis is focused on the speed error by calculating the RMSE and highlighting the observer performance. The implementation of the ALO algorithm is slightly more complicated compared to the implementation of the MRAS algorithm. The MRAS has fewer parameters to tune compared to ALO where both methods need to tune the adaptation mechanism. The no-load test demonstrates that the MRAS is more accurate compared to ALO. In the load test experiment, the MRAS and ALO have comparable performance in terms of accuracy and tracking. The experiments demonstrate a clear difference between the no-load and load RMSE values. Especially, the RMSE of MRAS increases in no-load compared to load tests, whereas the RMSE for ALO remains almost the same.

REFERENCES

[1] P. Vas, *"Sensorless Vector and Direct Torque Control."*, Oxford University Press, Oxford, 1998.

[2] J. You, W. Wu, and Y. Wang, "An Adaptive Luenberger Observer for Speed-Sensorless Estimation of Induction Machines.", 2018 Annual American Control Conference (ACC), pp. 307–312, 27-29 June 2018.

[3] Y. Zhang, Z. Zhao, T. Lu, L. Yuan, W. Xu, J. Zhu, "A comparative study of Luenberger observer, sliding mode observer and extended Kalman filter for sensorless vector control of induction motor drives.", 2009 IEEE Energy Conversion Congress and Exposition, pp. 2466–2473, 20-24 September 2009.

[4] J. Song, K. Lee, J. Song, I. Choy, K. Kim, "Sensorless vector control of induction motor using a novel reduced-order extended Luenberger observer.", Conference Record of the 2000 IEEE Industry Applications Conference. Thirty-Fifth IAS Annual Meeting and World Conference on Industrial Applications of Electrical Energy (Cat. No.00CH37129), pp. 1828–1834, 08-12 October 2000.

[5] M. Trabelsi, M. Jouili, M. Boussak, Y. Koubaa, M. Gossa, "Robustness and limitations of sensorless technique based on Luenberger state-Observer for induction motor drives under inverter faults.", 2011 IEEE International Symposium on Industrial Electronics, pp. 716–721, 27-30 June 2011.

[6] T. Pană, O. Stoicuţa, "Design of an extended luenberger observer for sensorless vector control of induction machines under regenerating mode.", 2010 12th International Conference on Optimization of Electrical and Electronic Equipment, pp. 469–478, 20-22 May 2010.

[7] P. Vaclavek, P. Blaha, "Lyapunov-function-based flux and speed observer for AC induction motor sensorless control and parameters estimation.", IEEE Transactions on Industrial Electronics, vol. 53, pp. 138 – 145, 06 February 2006.

[8] C. Ta, T. Uchida, Y. Hori, "MRAS-based Speed Sensorless Control for Induction Motor Drives Using Instantaneous Reactive Power." IECON'01. 27th Annual Conference of the IEEE Industrial Electronics Society (Cat. No.37243), pp. 1417–1422, 29 November 2001 - 02 December 2001.

[9] Andrew N. Smith, Shady M. Gadoue, John W. Finch, "Improved Rotor Flux Estimation at Low Speeds for Torque MRAS-Based Sensorless Induction Motor Drives.", IEEE Transactions on Energy Conversion, vol.31, pp.270 - 282, 15 October 2015.

[10] T. Orlowska-Kowalska, M. Dybkowski, "Stator-Current-Based MRAS Estimator for a Wide Range Speed-Sensorless Induction-Motor Drive.", IEEE Transactions on Industrial Electronics, vol. 57, pp. 1296 - 1308, April 2010.

[11] Y. B. Zbede, S. M. Gadoue, D. J. Atkinson, "Model Predictive MRAS Estimator for Sensorless Induction Motor Drives.", IEEE Transactions on Industrial Electronics, vol. 63, pp. 3511 - 3521, June 2016.

[12] C. Schauder, "Adaptive Speed Identification for Vector Control of Induction Motors without Rotational Transducers.", IEEE Transactions on Industry Applications, vol. 28, pp. 1054 - 1061, Sept.-Oct. 1992.

[13] NXP Semiconductors, *"Sensorless ACIM Field-Oriented Control."*, 2021.

[14] B. Ufnalski, L. Grzesiak, "Selected Methods in Angular Rotor Speed Estimation for Induction Motor Drives.", EUROCON 2007 - The International Conference on "Computer as a Tool", pp. 1764 - 1771, 09-12 September 2007.

[15] Ahmad Razani Haron, Nik Rumzi Nik Idris, "Simulation of MRAS-based Speed Sensorless Estimation of Induction Motor Drives using MATLAB/SIMULINK.", 2006 IEEE International Power and Energy Conference, pp. 411 - 415, 28-29 November 2006.

[16] S. Gadoue, D. Giaouris, J. Finch, "An experimental assessment of a stator current MRAS based on neural networks for sensorless control of induction machines.", EUROCON 2007 - 2011 Symposium on Sensorless Control for Electrical Drives, pp. 102 - 106, 01-02 September 2011.